Dynamic Non-Linear Skin Friction of Piles

Frottement Latéral Dynamique Non-Linéaire des Pieux

A. HOLEYMAN Ir., M.S., Dr., Assistant Manager, Research and Geotechnics, S.A. Franki N.V., Part-time Assistant Professor, Université Libre de Bruxelles, Belgium

SYNOPSIS A rational procedure to model the dynamic non linear behaviour of the skin friction of piles during driving is presented. It rests on the fundamental analysis of the embedded cylinder in a semi infinite medium. The static model suggested by Randolph and Wroth, which can accomodate heterogeneity is investigated under dynamic behaviour. The model is extended in the field of large deformations, with the adoption of a simple hyperbolic stress-strain law. Basic consideration under static loading conditions shows that the plastic zone around the pile remains very localized. This observation is enhanced in the dynamic case.

1. SCOPE.

The lateral friction acting along a pile during driving is not yet very well understood. In the model proposed by E. Smith (1960) for wave equation analyses, it is locally represented by a single degree of freedom system, with the recognized parameters : ultimate "static" skin friction τ_f, quake s_f and damping constant J_f. Whereas the skin friction can be related to in-situ tests or other means of designing piles, the quake and mainly the damping constant are rather mysteriously chosen. Some correlations exist between these last two parameters and the nature of the soil but the scatter is very large.

The attempt to rationally choose these important parameters beforehand consists in the following steps :
- examine the problem under static condition to define some spring constant,
- examine the problem under harmonic behaviour,
- generalize the available solutions to the case of large deformations.

When developing this approach, we shall see that each parameter used has a physical meaning and can be determined experimentally by other means.

2. THEORIES AVAILABLE FOR SMALL STRAINS.

Although soil does not behave elastically, it can be reasonnably assumed that for small strains, use could be made of the available solutions existing in elasticity. Although subsoil is heterogeneous, a cylindrical pile embedded in a homogeneous isotropic elastic half space will be considered at first, with the following characteristics :

pile : - R radius of the pile
- D depth of embedment

medium : - G shear modulus
- ν Poisson's ratio

2.1. Static case.

Among the available solutions relating to skin friction, we shall adopt the uncoupled model suggested by Randolph and Wroth (1978). These authors visualize the behaviour of the medium by separating it into : (Fig. 1)
- a half-space taking care of the base resistance
- a layer of depth D, taking care of the friction.

The pile is rigid and the displacement u_s of its shaft is obtained by integration of the angular distortion of the concentric cylinders surrounding the pile. Assuming that the variation of the vertical stress induced by the vertical displacement of the pile can be neglected and that the layer must be limited to a cylindrical boundary, at radius R_m, they obtain a simple and finite answer :

$$u_s = \frac{\tau_s R}{G} \ln \left(\frac{R_m}{R}\right) \qquad (1)$$

in which τ_s is the constant shear stress mobilized along the shaft.

Taking into account the compatibility of the displacement induced at the bottom of the layer and at the surface of the lower half-space, they suggest to adopt the following value for the fixed boundary radius :

$$R_m = 2.5\ D\ (1-\nu) \qquad (2)$$

Introducing in a further step the compressibility of the pile, these authors obtain answers very similar to those resulting from an integral equation analysis. Recommandations are given to handle heterogeneous media by introducing a corrected influence radius.

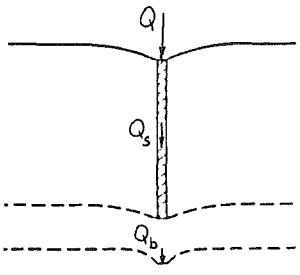

Fig. 1 : Uncoupled model

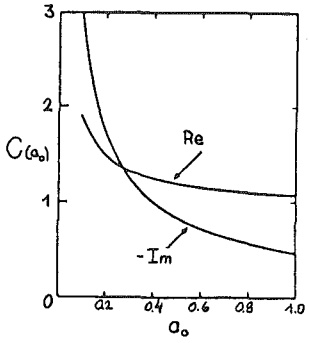

Fig. 2 : Impedance coefficient

2.2. Dynamic case.

Some assumptions are necessary to obtain a closed form solution :
- the pile is infinite
- the pile is rigid.

Under these circumstances, the problem becomes one-dimensional and the basic solution consists of cylindrical shear waves travelling in the radial directions. Baranov (1967) gives the fundamental differential wave equation whose solution can be expressed according to Kuhlemeyer (1979) in the form :

$$\tau_{rz} = C_h \cdot \frac{\partial u}{\partial t} \qquad (3)$$

with τ_{rz}: shear stress, u : vertical displacement, and with :

$$C_h = \rho v_s \, C(a_o)$$

a_o is the well known adimensional frequency :

$$a_o = \frac{\omega r}{v_s} \qquad (4)$$

with ω the frequency of the harmonic movement and r the current radial distance.

The coefficient C_h is the specific impedance of the infinite medium relative to the movement of the considered cylinder. ρv_s represents the specific impedance of a half-space relative to plane shear waves. The ratio of these two impedances is the coefficient $C(a_o)$, which is represented in fig. 2 as a function of a_o. It can be seen that for large values of a_o, the imaginary part vanishes whereas the real part of $C(a_o)$ tends to one : in that case the action of an infinite medium can be approximated by the one produced by a dashpot at a radius large enough such that a_o reaches a sufficient value. On the other hand, for small values of a_o, the behaviour is getting more similar to the static case for which the displacement becomes infinite. To obtain a finite displacement, the introduction of a radius of influence or a similar effect will be therefore required.

3. LARGE STRAINS.

3.1. Hyperbolic model.

A simple law, yet progressively introducing plasticity, can be used to handle large deformations : it is the hyperbolic law, relating shear stress τ to the shear deformation γ (Kondner, 1963). Introducing τ_f the ultimate shear strength and $\gamma_r = \tau_f/G_i$ the reference shear deformation, the law can be expressed as follows :

$$\frac{\gamma}{\gamma_r} = \frac{\eta}{1-\eta} \qquad (5)$$

with $\eta = \tau/\tau_f$, mobilization ratio.
G_i = initial tangent shear modulus.

Its graphical representation (fig. 3) shows the almost elastic aspect for small strains and its almost purely plastic aspect for very large strains.

3.2. Static case

For the infinitely long, incompressible pile considered in paragraph 2.1, the shear stress distribution is uniform along concentric cylinders and the displacement profile can be obtained by direct integration of the angular distortion, from the radius of influence R_m to the radius of the pile R :

$$u_s = \int_R^{R_m} \gamma dr = \int_R^{R_m} \frac{dr}{\frac{G_i r}{\tau_s R} - \frac{1}{\gamma_r}}$$

$$= \frac{R\tau_s}{G_i} \ln \frac{R_m/R - \eta_s}{1 - \eta_s} \qquad (6)$$

with $\tau_s = \tau_{rz}$ at $r = R$

$\eta_s = \tau_s/\tau_f$

To study the non-linear behaviour of the shaft, expression (6) has been represented in fig. 3 in an adimensional form :

$$\frac{u_s}{u_{sr}} = \frac{u_s \, G_i}{R \, \tau_f \ln (R_m/R)} = \eta \, \frac{\ln \frac{R_m/R - \eta_s}{1 - \eta_s}}{\ln (R_m/R)}$$

for $\ln R_m/R = 5$ (e.g R_m= 30 m and R = 0.21 m), as a function of the mobilization ratio at the shaft η_s. One can notice that for very small mobilization ratios, the behaviour is similar to the one given by the intrinsic adimensional law. However, as the mobilization ratio increases, the behaviour is stiffer than the intrinsic law up to $\eta_s \simeq 0.95$, above which the curve plunges more abruptly. This is the sign of a localized failure zone, limited to the vicinity of the shaft.

To visualize the extent of the large plastic deformations, displacement profiles have been represented in fig. 4 as functions of the radius for different mobilization ratios. Adimensional parameters have been chosen to give a general picture : the normalized displacement

$$\frac{u_s \, G_i}{R\tau_s} = \ln \frac{R_m/R - \eta_s}{1 - \eta_s}$$

has been represented as a function of $\ln R_m/R$.

As any value of R_m can be taken in this expression, the function represents the vertical displacement difference between the shaft and at any radial distance.

It can be seen that for small values of the mobilization ratio, the settlement profile is

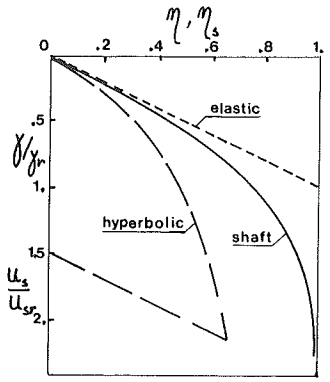

Fig. 3 : deformation curves

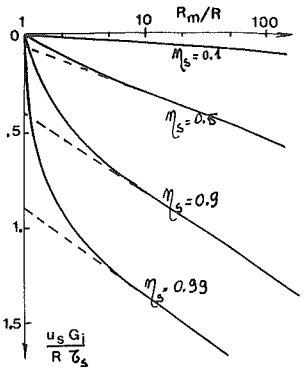

Fig. 4 : settlement profiles.

linear in this semi-logarithmic graph and relates to the quasi-elastic behaviour of the layer. As the mobilization ratio increases, the displacement gradient becomes larger in the vicinity of the pile (R_m /R = 1) whereas at some distance from the pile shaft the linear trend is found again. This trend corresponding to the elastic behaviour is prolonged by a dotted line whose intercept with the vertical axis is a measure of the plastic deformation of the shaft. This plastic increment represents a major part of the settlement for $\eta > 0.9$ for usual values of R_m/R and is independent of R_m/R provided $R_m/R \geq 5$ to 10. One can therefore conclude from such profiles that plasticity is confined within one to two radii from the shaft surface and that the behaviour will be faithfully represented if the soil is considered to behave elastically beyond 10 radii from the shaft surface.

3.3. Dynamic case.

For this case, the necessary numerical integration of the equations of movement is similar to the one suggested by Smith, but transposed in the radial direction. The layer is discretized into concentric cylinders (Fig. 5a) which are lumped into mass and stiffness parameters (Fig. 5b). Each mass is allowed to move vertically whereas the stiffness restraining their relative movement is the shear stiffness between cylinders.

In order to limit the extent of the modelled layer, at its outer boundary a condition according to eq. (3) can be adopted. In particular, if a_o is sufficiently large ($a_o \geq 8$ for example), a dashpot with a damping constant

$$C_\ell = 2\pi R_m \sqrt{G\rho} \qquad (7)$$

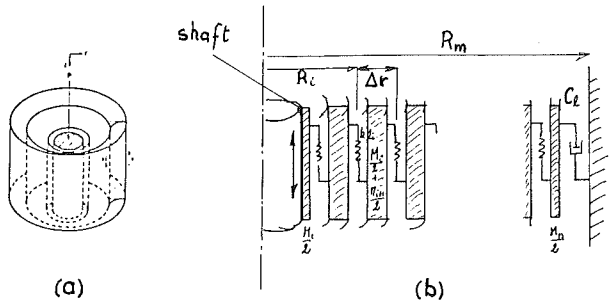

Fig. 5 : discretized model.

can be adopted to model the behaviour of the boundary at $R = R_m$.

4. NUMERICAL RESUTLS

4.1. Unbounded homogeneous elastic medium.

The problem treated in the case of an elastic medium has the following characteristics, chosen for the simplicity of the adimensional parameters :

$R = 1$ m
$G = 5$ MPa
$\rho = 0.002$ Mkg/m^3
$R_m = 20$ m
$\Delta r = 0.25$ m

$v_s = 50$ m/s
$a_o = \omega/50$

For such geometric conditions, the elastic displacement of this shaft vertically loaded by static force T = 10.487 MN per linear meter is according to (1) :

$$u_s = \frac{10.487}{2\pi.5} \ln \left(\frac{20}{1}\right) = 1 \text{ m.}$$

To be able to examine the effect of the pile mass on its harmonic behaviour, the adimensional mass parameter is defined :

$$b' = \frac{M_\ell}{\rho \pi R^2}$$

Where M_ℓ is the linear mass of the pile. This mass is added in the model at the boundary between the shaft and the soil. In practice, b' can vary between 0.5 and 1.5 and a typical case is b' = 1.

The amplitude u_o of the harmonic movement is obtained by exerting a sinusoïdal force of the mentioned amplitude (T_o= 10.487 MN) at the shaft and by reading out the peak displacements when the movement becomes periodic. This straightforward procedure can be kept for the non elastic case.

Results are presented in fig. 6 : the dynamic magnification factor M as a function of the adimensional frequency a_o. The magnification factor is conventionally defined by :

$$M = u_o/u_s \qquad (8)$$

For the massless shaft (b' = o), the curve is regular for the larger values of a_o and some riples are observed for $a_o < 0.4$ as could be anticipated. It is compared with the almost exact solution proposed by Novak (1972), following the work of Baranov (1967).

One can notice that the modellization gives results in close agreement with the standard solution, and clearly in particular for $a_o > 0.4$ The effect of adding mass to the shaft is to increase the displacement amplitude for lower frequencies and decrease it for higher frequencies.

4.2. Harmonic behaviour of non-linear medium.

The problem treated for the non-elastic case is characterized by the same parameters as the one dealt in paragraph 4.1, except that the ultimate shear strength τ_f is chosen in relation to the amplitude T_o of the vertical force. The

mobilization ratio is indeed :

$$\eta_s = \frac{T_o}{2\pi R\ \tau_f} \qquad (9)$$

Results of the computed cases are given in fig. 7 for various values of the mobilization ratio. The continuous lines correspond to an outer boundary condition according to expression (7). It is therefore assumed that, at 20 radii from the axis of the pile, the stress level is low enough to consider that the soil behaves practically as an elastic body. This value of R_m/R is indeed larger than the one observed for the static case (fig. 4).

This model apparently behaves reasonably well but misses one of the requirements of a wave equation analysis including the assessment of the residual stresses. These can only be computed by finding the equilibrium position of the pile after its larger displacements and to obtain any residual stress, a static stiffness is required. It is not the case of the present model because the adopted dashpot at the boundary does not behave reallistically at very low frequencies. On the other hand, to fulfill the static displacement condition according to the Randolph and Wroth theory, one must fix the boundary cylinder.

This calculation has also been performed, but with a zero displacement condition at radius R_m. These results are given by dots also in fig. 7 for $\eta_s = 1$ and $\eta_s = 2$. It is obvious that for low stress mobilization, the quasi-elastic behaviour of the modelled volume is influenced by reflections from the fixed outer boundary and the solutions computed with both conditions (dashpot or fixed) vastly differ. It is interesting to note however that for large mobilization ratios, the effect of the choice of the boundary condition vanishes. For $\eta_s = 1$ the dots come within 10 % of the continuous line whereas for $\eta_s = 2$, the agreement between both problems becomes amazing. This is once more the evidence that a plastic zone, localized in the close vicinity of the pile shaft is governing the behaviour of the pile, and that one conclusion from the static analysis can be generalized in the case of the harmonic behaviour. Plastic wave do not propagate very far from the pile shaft.

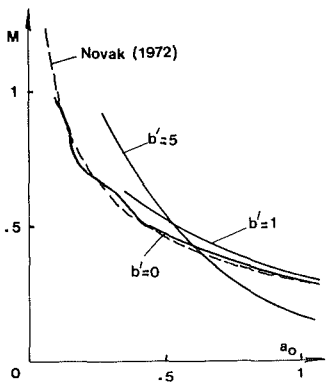

Fig. 6 : elastic medium

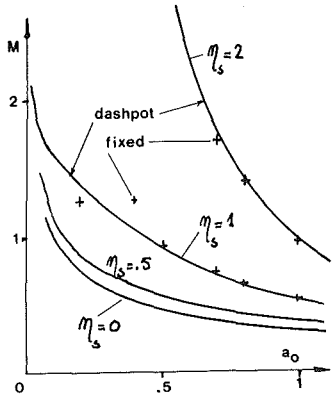

Fig. 7 : non elastic medium

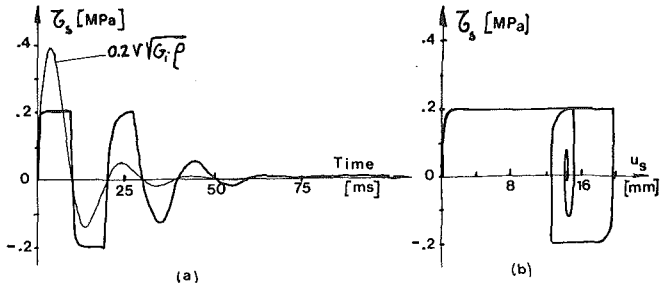

Fig. 8 : (a) Stress-time diagram
(b) Stress-displacement diagram

4.3 Transient behaviour during driving.

During driving, the soil around the shaft is sollicited well above its shear strength as will be seen below and one can consider the transient condition as a displacement condition at the shaft interface. As an example, we shall study the shear stress mobilized at a pile shaft with R = 0.3 m whose movement is described by its speed v :

$$v = v_o\ e^{-\alpha t} \sin \omega t \qquad (10)$$

and we shall adotpt : v_o = 5 m/s, ω = 100 s^{-1} and ω = 3/4 rad/sec (50 Hz)

Results presented in fig. 8.a. and b. correspond to a quite high value of τ_f = 0.2 MPa for a medium characterized by G_i = 187 MPa (E_i = 500 MPa and ν = 1/3) and ρ = 0.002 Mkg/m^3. In the first figure is shown the stress τ at the shaft as a function of time, along with its the velocity multiplied by a fifth of the specific plane shear impedance (0.2 v . $\sqrt{G\rho}$). In the second one, the mobilized stress is given as a function of the displacement of the shaft.

One can notice the strong effect of impedance, bringing the stress almost instantaneously up to the ultimate. This is the influence of the geometrical damping. The hysteretic damping on the other hand is handled by the use of the intrinsic hyperbolic stress-strain law. Viscous behaviour could be included. At last, a velocity dependent law could also be adopted for the ultimate value of the shear stress. One can perceive the physical insight afforded by this model and therefrom conceive equivalent single degree of freedom systems.

5. REFERENCES.

HOLEYMAN A., (1984), "Contribution à l'Etude du Comportement Dynamique Non-Linéaire des Pieux lors de leur Battage, Doctoral Thesis, Université Libre de Bruxelles, ICC, July, 584 p.

KUHLEMEYER R.L., (1979), "Vertical Vibration of Piles", J. Geot. Eng. Div., Proc. ASCE 105 N° GT2, Feb. 1979, pp. 273-287.

RANDOLPH M.F. & WROTH C.P., (1978), "Analysis of Deformation of Vertically Loaded Piles", ASCE, Jrl. of the Geotechnical Division, Vol. 104, N° GT12, December 1978, pp. 1465-1488.